Binding of Tachyplesin I to DNA Revealed by Footprinting Analysis: Significant Contribution of Secondary Structure to DNA Binding and Implication for Biological Action†

Atsuo Yonezawa,‡ Jun Kuwahara,‡ Nobutaka Fujii,§ and Yukio Sugiura*,‡

Institute for Chemical Research, Kyoto University Uji, Kyoto 611, Japan, and Faculty of Pharmaceutical Sciences, Kyoto University, Kyoto 606, Japan

Received September 24, 1991; Revised Manuscript Received December 31, 1991

ABSTRACT: In view of the cationic amphipathic structure of tachyplesin I and antiparallel β-sheet as a general DNA binding motif, DNA binding of the antimicrobial peptide has been examined. Several footprinting-like techniques using DNase I protection, dimethyl sulfate protection, and bleomycin- (BLM-) induced DNA cleavage were applied in this study. Some distinct footprints with DNase I are detected, and also the sequence-specific cleavage mode of the BLM–Fe(II) complex clearly is altered in the presence of tachyplesin I. In addition, methylation of the N-7 residue of guanine situated in the DNA major groove is not entirely inhibited (or activated) by tachyplesin I. The results suggest that tachyplesin I interacts with the minor groove of DNA duplex. Disappearance of the footprints by dithiothreitol-treated tachyplesin I and Ala–tachyplesin strongly suggests a significant contribution of secondary structure containing an antiparallel β-sheet to the DNA binding of tachyplesin I. This is the first report on DNA interaction with a small peptide which contains a unique antiparallel β-sheet structure. The mechanism for antimicrobial action of tachyplesin I has also been inferred.

Tachyplesin I, an antimicrobial cationic peptide, was isolated from the hemocyte membrane of Japanese horseshoe crab (*Tachypleus tridentatus*) in 1988 (Nakamura et al., 1988). The peptide has an unusual structure containing 17 amino acid residues with a carboxyl-terminal arginine α-amide (Figure 1A). A recent ^{1}H NMR study showed that tachyplesin I takes on a fairly rigid conformation constrained by two disulfide bridges and adapts a conformation consisting of an antiparallel β-sheet (residues 3–8 and 11–16) connected by a β-turn (residues 8–11) (Kawano et al., 1990). This planar conformation model reveals a distinct dichotomy between the two sides of the β-sheet; namely, on one side there is a large cluster of bulky hydrophobic side chains while on the other side there is a pair of charged guanidinyl side chains (Figure 1B). It is suggested that the unique structure of tachyplesin I may play an important role in the interaction between the peptide and LPS (Nakamura et al., 1988; Miyata et al., 1989).

In view of the cationic amphipathic β-sheet structure of tachyplesin I and the antiparallel β-sheet as general DNA binding motif (Rafferty et al., 1989; Yang & Nash, 1989; Breg et al., 1990; Scherly et al., 1990; Churchill & Travers, 1991; Hoffman et al., 1991), it is of special interest to examine DNA interaction with tachyplesin I. Therefore, we first investigated the binding between tachyplesin I and DNA by using several footprinting techniques such as DNase I[1] protection (Galas & Schmitz, 1978), DMS protection (Siebenlist & Gilbert, 1980), and alteration of sequence-specific cleavage by the BLM–Fe(II) complex (Sugiura & Suzuki, 1982). Tachyplesin I (reduced form) and Ala–tachyplesin (Figure 1A) were also tested to clarify the significant contribution of the unique secondary structure of tachyplesin I to DNA binding. Herein, we found that tachyplesin I clearly interacts in the DNA minor groove and that the rigid antiparallel β-sheet structure of tachyplesin I plays an important role for DNA binding of the peptide.

Experimental Procedures

Materials. Tachyplesin I and Ala–tachyplesin were synthesized and purified as described previously (Akaji et al., 1989). *Fok*I restriction endonuclease was a kind gift of Drs. M. Takanami and H. Sugisaki (Kyoto University). DNase I and *Eco*RI were obtained from Takara Shuzo (Kyoto, Japan). The second generation BLM, peplomycin (PEM), was supplied by Nippon Kayaku. All other chemicals used were of commercial reagent grade.

DNase I Footprinting Analysis for Tachyplesin I and Its Analogue. Each reaction mixture (final volume 20 μL) contained 20 mM Tris-HCl buffer (pH 7.5), 5 mM $CaCl_2$, 10 mM $MgCl_2$, tachyplesin I or its analogue, and the ^{32}P-end-labeled 134-bp DNA fragment (pIBI24 *Eco*RI–*Fok*I), in which the final amount was made up to 660 pmol (base pairs) by addition of sonicated CT DNA. After incubation at 20 °C for 30 min, the sample was digested with DNase I (final concentration 1 unit/mL) for 2 min. In order to stop the reaction, 5 μL of DNase I stop solution (250 mM Na_2EDTA and 3 M sodium acetate) and 60 μL of cold ethanol were added to the sample solution. Electrophoresis was performed in a 10% polyacrylamide/7 M urea slab gel at 2000 V for 2 h. After electrophoresis, an autoradiogram was made by ^{32}P-end-labeled DNA in the gel. DNA sequencing was carried

† This study was supported in part by a Grant-in-Aid for Scientific Research on Priority Areas from the Ministry of Education, Science, and Culture of Japan.

* Author to whom correspondence should be addressed.
‡ Institute for Chemical Research, Kyoto University.
§ Faculty of Pharmaceutical Sciences, Kyoto University.

[1] Abbreviations: BLM, bleomycin; CD, circular dichroism; DNase I, deoxyribonuclease I; Na_2EDTA, disodium ethylenediaminetetraacetate; DTT, dithiothreitol; CT DNA, calf thymus DNA; DMS, dimethyl sulfate; *cis*-DDP, *cis*-diamminedichloroplatinum; UV, ultraviolet; IHF, integration host factor; RNP, U1 small nuclear ribonucleoprotein; LPS, lipopolysaccharide.

0006-2960/92/0431-2998$03.00/0

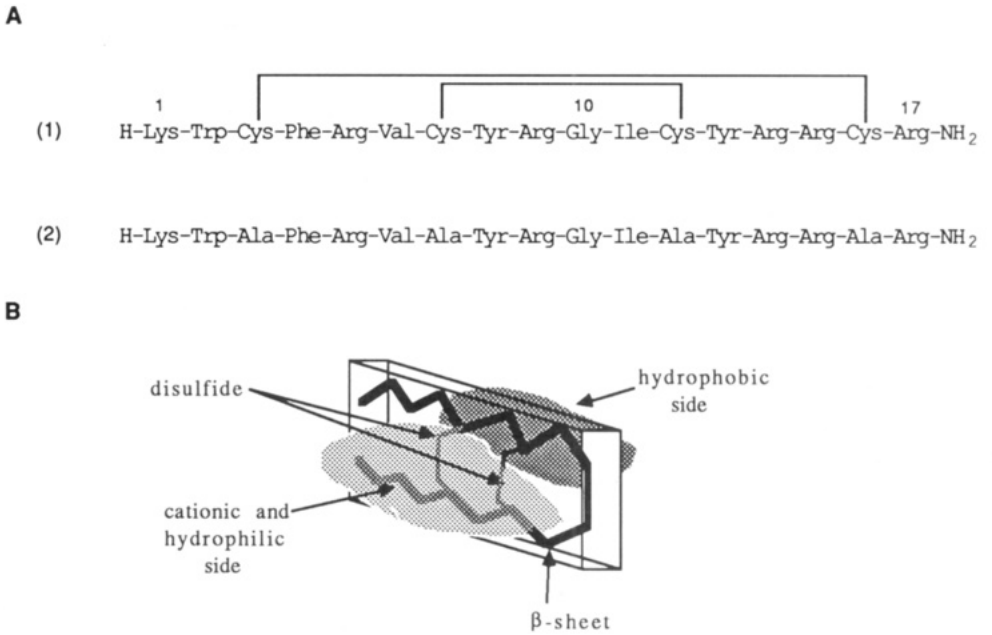

FIGURE 1: (A) Primary structures of tachyplesin I (1) and Ala-tachyplesin (2). (B) Model for secondary structure of tachyplesin I.

out by the Maxam–Gilbert method (Maxam & Gilbert, 1980). The radioactivity of each sample subjected to electrophoresis was approximately 15 000 cpm.

DNase I Footprinting Analysis for Tachyplesin I in the Presence of a Thiol Compound. Tachyplesin I was preincubated with 150 μM (7-fold excess) DTT in the reaction buffer [20 mM Tris-HCl buffer (pH 7.5), 5 mM $CaCl_2$, and 10 mM $MgCl_2$] at 20 °C for 15 min, and then the ^{32}P-end-labeled 134-bp DNA fragment (pIBI24 *Eco*RI–*Fok*I) was added to the reaction mixture. After incubation at 20 °C for 30 min, the DNA was digested by addition of DNase I (2×10^{-2} units). The DNA digestion was stopped by addition of the DNase I stop solution (5 μL) and cold ethanol (60 μL) after 2 min. Electrophoresis was performed in a 10% polyacrylamide/7 M urea slab gel at 2000 V for 2 h. The radioactivity of each sample subjected to electrophoresis was approximately 15 000 cpm.

Alteration of BLM–Fe(II) Complex-Induced DNA Cleavage by Tachyplesin I. The reaction mixture (final volume 20 μL) contained tachyplesin I, the ^{32}P-end-labeled 134-bp DNA fragment (pIBI24 *Eco*RI–*Fok*I), sonicated CT DNA (660 pmol), and 20 mM Tris-HCl buffer (pH 7.5). After preincubation at 20 °C for 30 min, the sample was digested with freshly prepared PEM–Fe(II) complex (final concentration 10 μM) for 15 min. The reaction was terminated by addition of 10 mM Na_2EDTA (2 μL), 3 M sodium acetate (2 μL), and 60 μL of cold ethanol. Electrophoresis was carried out according to the method given for DNase I footprinting analysis for tachyplesin I.

DMS Protection Analysis. The reaction mixture (final volume 20 μL) contained the ^{32}P-end-labeled 134-bp DNA fragment (pIBI24 *Eco*RI–*Fok*I) and tachyplesin I in 20 mM Tris-HCl buffer (pH 7.5) containing 10 mM EDTA. After preincubation at 20 °C for 30 min, 10% DMS (1 μL) was added to the sample and then the sample solution was incubated for 5 min. The reaction was terminated by addition of 5 μL of DMS stop solution [1.5 M acetate buffer (pH 7.0), 1 M β-mercaptoethanol, and 250 μg/mL yeast tRNA] and 75 μL of cold ethanol. The DNA was recovered by centrifugation at 15 000 rpm for 10 min, and then the ethanol precipitation was carried out again. After being rinsed and dried, the sample was treated with piperidine at 90 °C for 30 min. Electrophoresis was performed under the conditions given for DNase I footprinting analysis for tachyplesin I.

CD Spectroscopic Measurement. CD spectra were recorded from 260 to 190 nm on a Jasco J600 spectropolarimeter at 20 °C. Tachyplesin I (50 μM) dissolved in 100 mM phosphate buffer (pH 7.5) was measured in the presence or absence of 350 μM DTT. Ala-tachyplesin (50 μM) was also measured in 100 mM phosphate buffer (pH 7.5).

RESULTS

DNase I Footprinting Analysis for Tachyplesin I. Figure 2 shows the autoradiogram of DNase I footprinting titration of tachyplesin I in the 5′-end-labeled pIBI24 *Eco*RI–*Fok*I restriction fragment (134 bp). From this autoradiogram, 55 bases were analyzed by the densitometer (nos. 14–69 from the *Eco*RI site). In comparison with the digestion by DNase I without tachyplesin I (lane 4), some footprints protected by tachyplesin I at 25 μg/mL (lane 7, solid arrow) and higher concentrations than 50 μg/mL (lanes 8–11, dotted arrow) were clearly detected. Figure 3 presents similar footprinting sites of tachyplesin I in the 3′-end-labeled complementary strand. The footprints of tachyplesin I for 55 bp of the 134-bp DNA fragment are summarized in Figure 5. The sites protected by tachyplesin I are located near base positions 15, 28, 38, and 48 and are also observed on both strands. In addition, the asymmetric footprinting pattern staggered by 2–4 base pairs to the 3′-side of DNA helix was observed. The result suggested that tachyplesin I interacts with DNA through contacts in the minor groove, as previously demonstrated with DNase I footprinting (Fox & Waring, 1984; Low et al., 1984).

Alteration of BLM–Fe(II) Complex-Induced DNA Cleavage by Tachyplesin I. Panels A and B of Figure 4 show the sequence-specific cleavage patterns by the BLM–Fe(II) complex in the presence or absence of tachyplesin I. Since this peptide is sensitive to reductants, DNA was cleaved by the BLM-Fe(II) complex at a higher concentration (final 10 μM) than under normal conditions without the use of DTT or H_2O_2. The BLM–Fe(II) complex alone preferentially cut duplex DNA at guanine–pyrimidine (5′ → 3′) sequences. In comparison with the control (lane 4), inhibition and enhancement of sequence-specific cleavage of DNA by the BLM–Fe(II) complex were evidently observed in the presence of tachyplesin

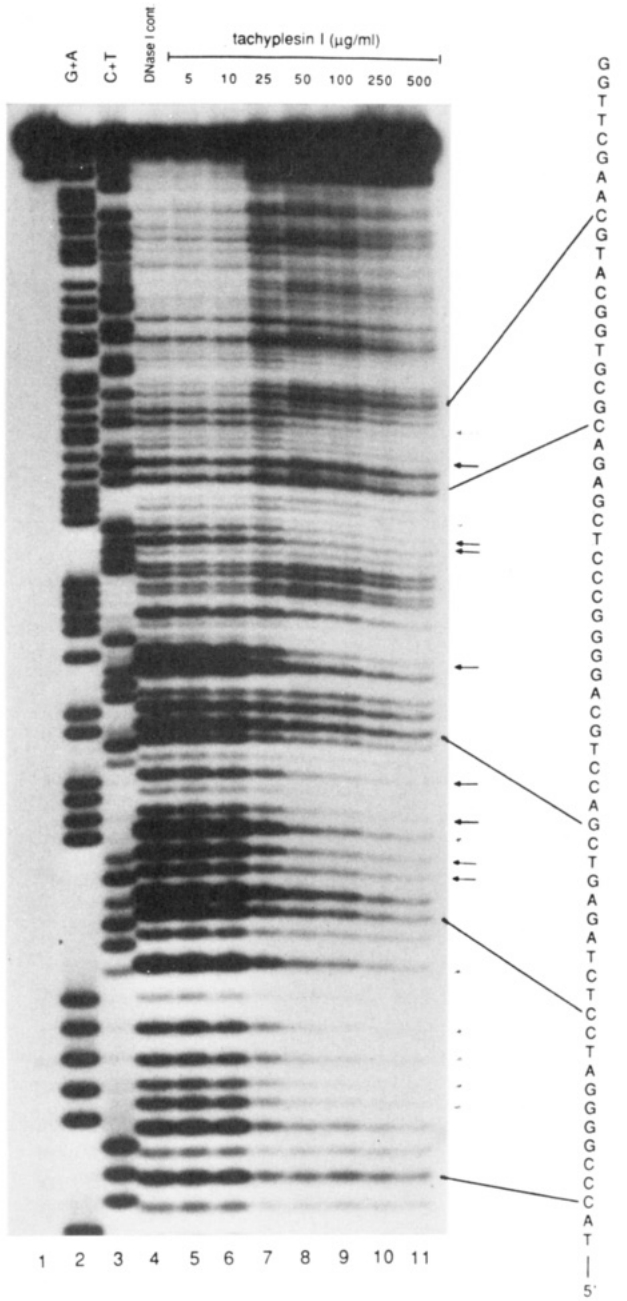

FIGURE 2: Autoradiogram of a 10% polyacrylamide gel for DNase I footprinting of tachyplesin I. The samples contained the following concentrations of tachyplesin I: lane 4, none; lane 5, 5 μg/mL (2.2 μM); lane 6, 10 μg/mL; lane 7, 25 μg/mL; lane 8, 50 μg/mL; lane 9, 100 μg/mL; lane 10, 250 μg/mL; and lane 11, 500 μg/mL. Lane 1 shows intact DNA alone. Lanes 2 and 3 exhibit DNA sequencing (G + A and C + T, respectively) by the Maxam–Gilbert method. From the autoradiogram of 5′-end-labeled DNA, 55 base pairs were analyzed by a densitometer. Solid and dotted arrows indicate the protection sites by tachyplesin I at 25 μg/mL (11 μM) and 50 μg/mL (22 μM), respectively.

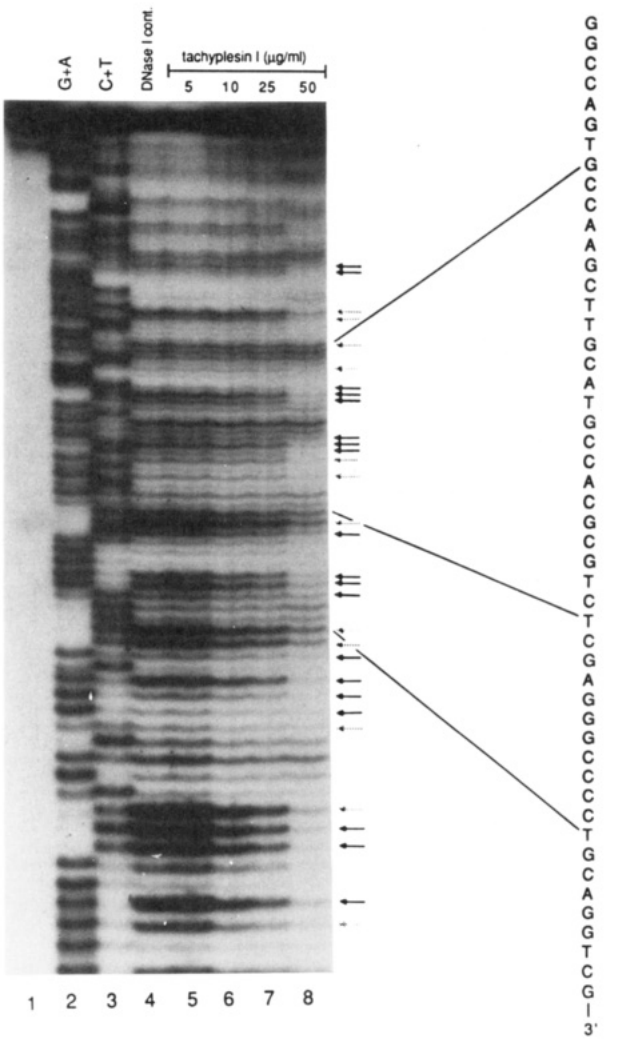

FIGURE 3: Autoradiogram of a 10% polyacrylamide gel for DNase I footprinting of tachyplesin I. The samples contained the following concentrations of tachyplesin I: lane 4, none; lane 5, 5 μg/mL (2.2 μM); lane 6, 10 μg/mL; lane 7, 25 μg/mL; and lane 8, 50 μg/mL. Lane 1 shows intact DNA alone. Lanes 2 and 3 exhibit DNA sequencing (G + A and C + T, respectively) by the Maxam–Gilbert method. From the autoradiogram of 3′-end-labeled DNA, 50 base pairs were analyzed by a densitometer. Solid and dotted arrows indicate the protection sites by tachyplesin I at 25 μg/mL (11 μM) and 50 μg/mL (22 μM), respectively.

I (lanes 5–7). Tachyplesin I at a higher concentration than 50 μg/mL significantly blocked DNA cleavage activity of BLM–Fe(II) complex. Figure 5 summarizes effect of tachyplesin I on DNA cleavage by the BLM–Fe(II) complex, together with the result by DNase I. In the presence of tachyplesin I, the altered sites correspond considerably well between the BLM–Fe(II) complex and DNase I systems.

DMS Protection Analysis. We also investigated DMS protection analysis (Siebenlist & Gilbert, 1980) to check whether tachyplesin I interacts through contacts with the DNA major groove or not. Tachyplesin I did not entirely inhibit or enhance methylation of the N-7 site of guanine residues situated in the DNA major groove (data not shown).

DNase I Footprinting Analysis for Tachyplesin I in the Presence of a Thiol Compound. The secondary structure of tachyplesin I is very sensitive to some reductants because of breakage of its disulfide bonds. Destruction of the secondary structure, the antiparallel β-sheet (Kawano et al., 1990), of tachyplesin I with a 7-fold excess of DTT was indeed observed by CD measurement (supplementary material). After tachyplesin I was preincubated with a 7-fold excess of DTT, therefore, DNase I footprinting was performed. Figure 6 shows the autoradiogram of DNase I footprinting of tachyplesin I for the 5′-end-labeled pIBI24 *Eco*RI–*Fok*I restriction fragment (134 bp) under this reducing condition. With consideration of the effect of DTT on DNase I activity, two DNase I controls with DTT (lane 4) and without the DTT (lane 7) were prepared. As shown in lanes 5 and 6, some cuttings of the bases protected by intact tachyplesin I were detected in the presence of DTT. Indeed, reduced tachyplesin I gave no clear footprints in the DNase I footprinting experiment.

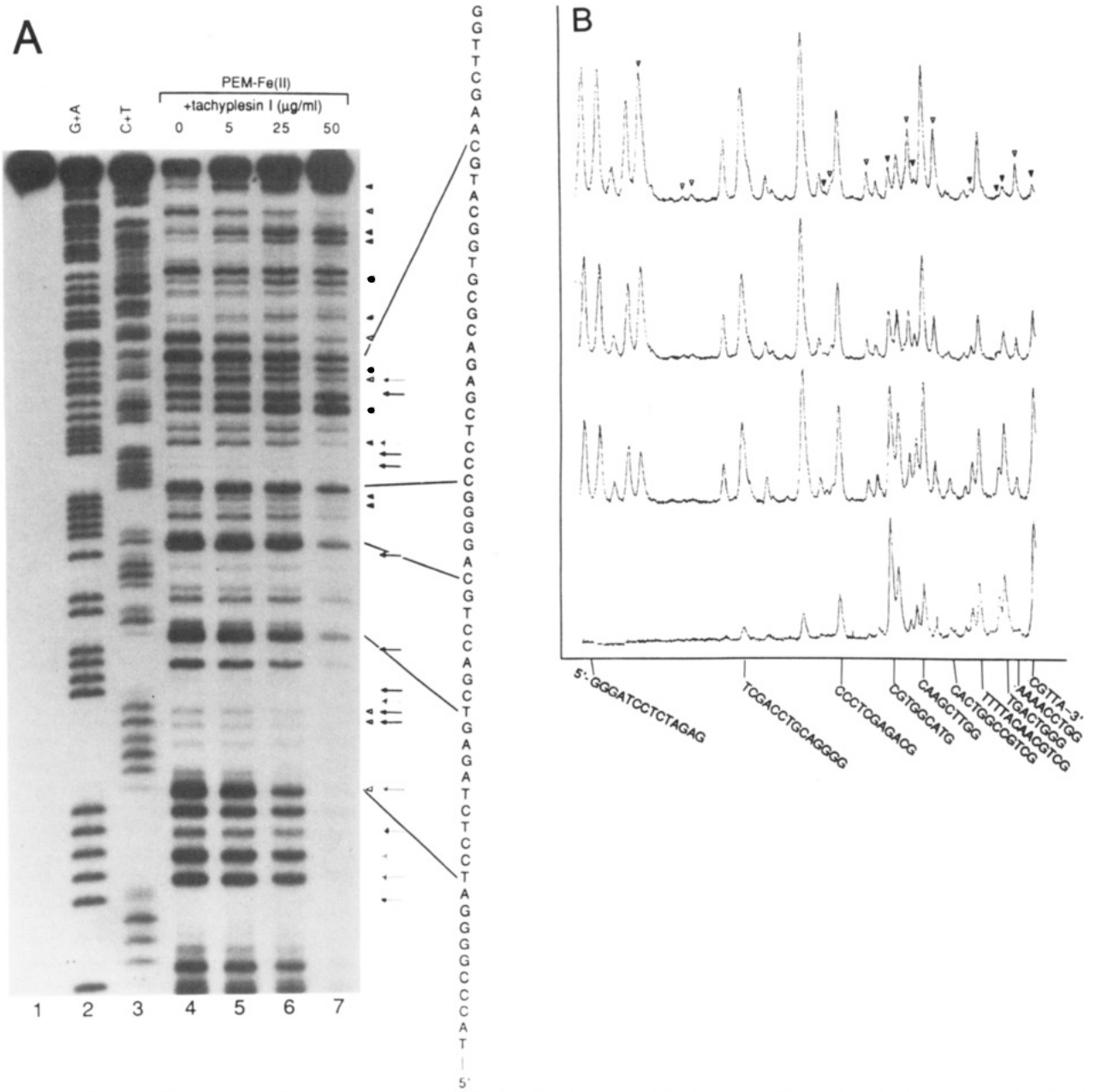

FIGURE 4: (A) Autoradiogram of a 10% polyacrylamide gel for DNA cleavage by the PEM–Fe(II) complex in the presence of tachyplesin I. The samples contained the following concentrations of tachyplesin I: lane 4, none; lane 5, 5 μg/mL (2.2 μM); lane 6, 25 μg/mL; and lane 7, 50 μg/mL. Lane 1 shows intact DNA alone. Lanes 2 and 3 exhibit DNA sequencing (G + A and C + T, respectively) by the Maxam–Gilbert method. From the autoradiogram of 5′-end-labeled DNA, 100 base pairs were analyzed by a densitometer. Open and closed triangles show the inhibited and enhanced cleavage sites by tachyplesin I, respectively. Arrows indicate the protection sites of tachyplesin I in the case of DNase I footprinting analysis. (B) Densitometric patterns of lanes 4–7 (top to bottom). The inhibited and enhanced cleavage sites are denoted by open and closed triangles, respectively.

DNase I Footprinting Analysis for the Tachyplesin Analogue. The CD spectrum of Ala–tachyplesin was apparently different from that of tachyplesin I (supplementary material). The DNase I footprinting experiment of the tachyplesin analogue, Ala–tachyplesin, was also performed carefully. No conspicuous footprints were observed in the case of Ala–tachyplesin (Figure 7).

Discussion

DNA Binding Property of Tachyplesin I. The footprinting technique (Galas & Schmitz, 1978) has been widely used to investigate sequence specificity of DNA binding compounds such as actinomycin D, echinomycin, distamycin, and the BLM–Co(III) complex (Van Dyke et al., 1982; Lane et al., 1983; Van Dyke & Dervan, 1983, 1984; Scamrov & Beabealashvilli, 1983; Low et al., 1984; Kuwahara & Sugiura, 1988). We demonstrated the DNA binding property of tachyplesin I by the use of DNase I footprinting analysis and the BLM–Fe(II) complex-induced DNA cleavage. When total DNA (CT DNA and 3′- or 5′-end-labeled DNA) was allowed to equilibrate with tachyplesin I at molar ratios (0.07–0.70) of tachyplesin I (50 μg/mL) to DNA base pairs, some distinct footprints consisting of the bases protected against DNase I digestion and apparent alteration of the BLM–Fe(II) complex-induced DNA cleavage pattern by tachyplesin I were observed. Considering the ratio of tachyplesin I to DNA, the peptide appears to bind to DNA no less strongly than other DNA binding peptides such as distamycin A and echinomycin (Van Dyke et al., 1982; Van Dyke & Dervan, 1984). Since synthetic tachyplesin I is used in this study, such a result is

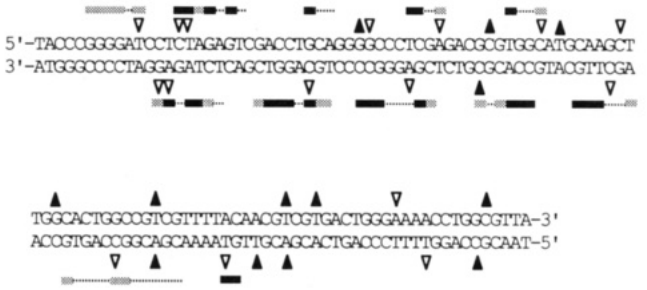

FIGURE 5: DNase I footprints of tachyplesin I determined from the autoradiograms of Figures 2 and 3 and alteration of BLM-induced DNA cleavage mode by tachyplesin I. Solid and shaded boxes show the results of DNase I footprinting with concentrations of 25 μg/mL (11 μM) and 50 μg/mL (22 μM) tachyplesin I, respectively. Open and solid triangles show the inhibited and enhanced cleavage sites of the BLM–Fe(II) complex, respectively.

not due to other contaminated proteins. In order to get more detailed information on the DNA binding site of tachyplesin I, we also applied the footprinting technique using small molecules such as (methidium-propyl)-EDTA–Fe(II) (Hertzberg & Dervan, 1982) or the Fe(II)–EDTA complex (Tullius et al., 1987). However, these DNA cleaving systems were inappropriate as footprinting reagents for tachyplesin I because of the requirement of a lot of reducing agent which destroys the secondary structure of tachyplesin I.

Distamycin A, netropsin, and Hoechest 33258 recognize AT-rich regions of DNA double strands (Van Dyke et al., 1982; Lane et al., 1983; Harshman & Dervan, 1985). Echinomycin and triostin A intercalate with CpG base pairs (Lane et al., 1983; Wang et al., 1984). From the footprinting result using the 346-bp fragment (*Bam*HI–*Hin*dIII) of pBR322 DNA, sequence-specific binding of tachyplesin I was not definitely observed. In the DNase I footprinting experiment of tachyplesin I for the 134-bp fragment of pBRZ24 DNA which contains AT- and GC-rich tracts, on the other hand, two footprints were detected on either side of the GC-rich tract. However, specific sequences involved in DNA binding of tachyplesin I were not demonstrated, although the peptide may recognize local structure of the DNA helix.

The interaction of DNA with tachyplesin I was investigated by a UV absorption method, and the electronic spectra in the range of 230–330 nm were almost identical between free tachyplesin and its DNA complex. Therefore, it appears that a direct intercalation involving aromatic amino acid residues (Trp, Tyr, Phe) and nucleic acid bases (Helene & Dimicoli, 1972; Morita, 1974) does not participate in the tachyplesin I–DNA interaction.

Plausible DNA Binding Mode of Tachyplesin I. The fact that metallobleomycin binds in the minor groove of B-DNA is supported by the following experimental results: (i) distamycin A changes the nucleotide sequence-specific cleavage mode of BLM (Sugiura & Suzuki, 1982); (ii) the 4′-hydrogen of deoxyribose abstracted by metallobleomycin situates in the DNA minor groove (Stubbe & Kozarich, 1987); (iii) the binding constant of the BLM–Co(III) complex is quite similar between glucosylated and nonglucosylated phage T4 DNAs; and (iv) in contrast to covalent attachment of guanine N-7 with aflatoxin B1, the modification of the guanine 2-amino group with anthramycin remarkably inhibits DNA cutting by metallobleomycin (Kuwahara & Sugiura, 1988). Evidently, tachyplesin I alters the DNA cleavage pattern by the BLM–Fe(II) complex. The facts strongly suggest that tachyplesin I interacts with DNA through contact with the minor groove. Some DNA binding compounds such as distamycin A, actinomycin D (Sugiura & Suzuki, 1982), anthramycin (Kuwahara & Sugiura, 1988), and *cis*-diamminedichloroplatinum (*cis*-DDP) (Mascharak et al., 1983) are known to alter the sequence-specific cutting mode by metallobleomycin. The effect of distamycin A, actinomycin D, or anthramycin is due to direct binding of these antibiotics to the DNA minor groove, whereas *cis*-DDP induces a drastic conformational change of the DNA double helix with its cross-linking and alters the DNA cleavage by metallobleomycin. Considering the facts that (i) DNase I footprints are staggered by 2–4 base pairs to the 3′-side of the DNA duplex, (ii) tachyplesin I does not inhibit (or enhance) the methylation of the N-7 of guanine residues situated in the DNA major groove, and (iii) the BLM–Fe(II) complex-induced DNA cleavage is changed by tachyplesin I, the peptide is indicated to be a minor groove binder of the DNA duplex. As DNase creates staggered cuts

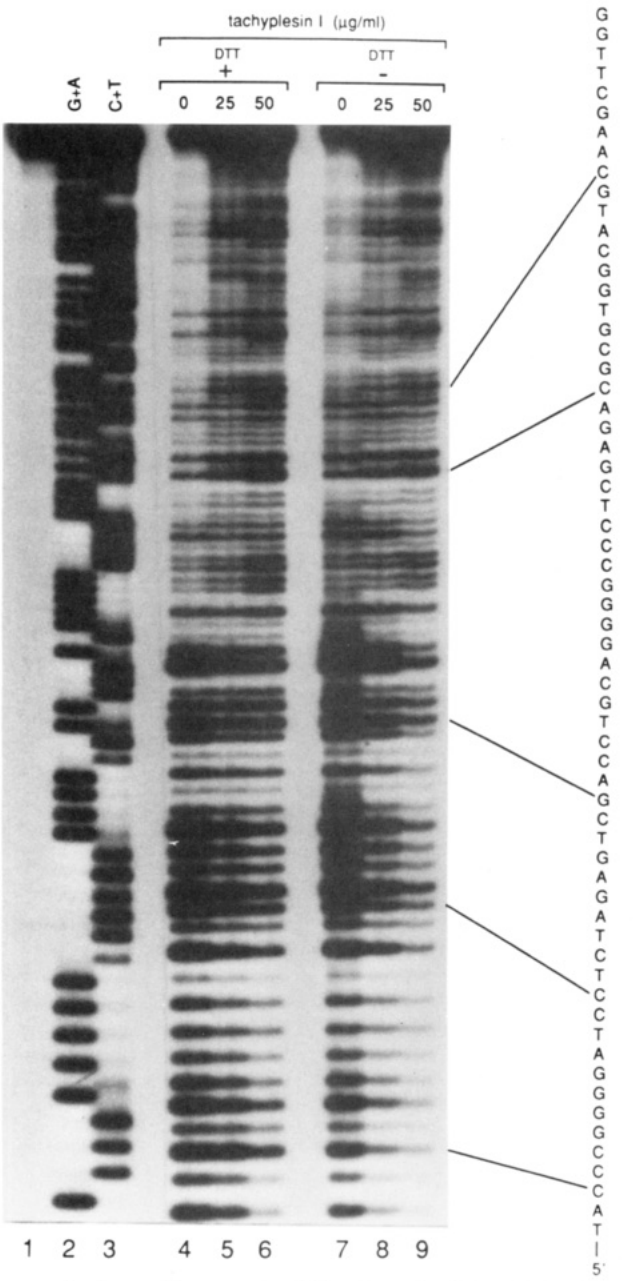

FIGURE 6: Autoradiogram of a 10% polyacrylamide gel for DNase I footprinting of DTT-treated (lanes 4–6) or intact (lanes 7–9) tachyplesin I. The samples contained the following concentrations of tachyplesin I: lanes 4 and 7, none; lanes 5 and 8, 25 μg/mL (11 μM); lanes 6 and 9, 50 μg/mL (22 μM). Lane 1 shows intact DNA alone. Lanes 2 and 3 exhibit DNA sequencing (G + A and C + T, respectively) by the Maxam–Gilbert method.

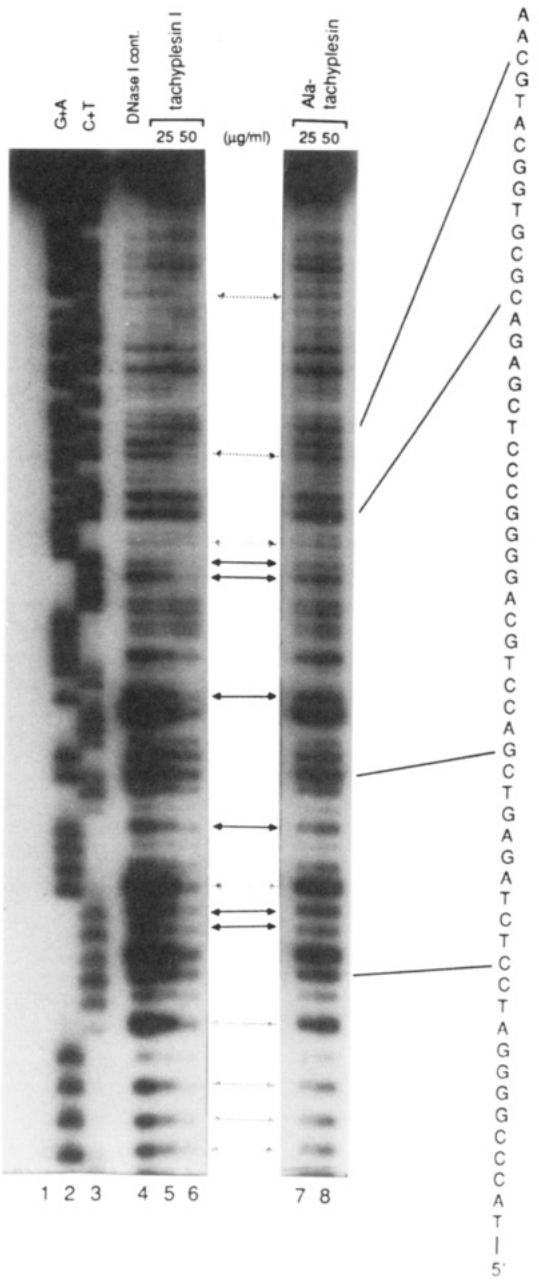

FIGURE 7: Autoradiogram of a 10% polyacrylamide gel for DNase I footprinting of Ala–tachyplesin (lanes 7 and 8) or tachyplesin I (lanes 5 and 6). The samples contained the following concentrations of Ala–tachyplesin or tachyplesin I: lane 4, none; lanes 5 and 7, 25 μg/mL (11 μM), lanes 6 and 8, 50 μg/mL (22 μM). Lane 1 shows intact DNA alone. Lanes 2 and 3 exhibit DNA sequencing (G + A and C + T, respectively) by the Maxam–Gilbert method.

not only in the minor but also in the major groove, it should be noted here that the staggered DNase footprints are not clearcut evidence for minor groove binding.

Importance of the Secondary Structure of Tachyplesin I for DNA Binding. Of special interest is the fact whether the unique secondary structure of tachyplesin I, an amphipathic β-turn-connected β-sheet, is essential or not for DNA binding activity of tachyplesin I. When the peptide was treated with DTT to cleave its disulfide bonds, the alteration of its secondary structure (disappearance of the β-sheet structure) and remarkable decline of DNA binding affinity were observed. The result reveals that (i) two disulfide bonds of tachyplesin I play an important role for maintenance of its secondary structure and (ii) the unique rigid β-sheet structure significantly influences DNA binding of the peptide. Indeed, the replacement of four cysteines by alanines in tachyplesin I led to a change of the secondary structure and to a decrease of the DNA binding affinity. These results strongly indicate a significant contribution of the secondary structure containing an antiparallel β-sheet to the DNA binding of the peptide.

The antiparallel β-sheet of tachyplesin I may attract keen attention in connection with the DNA binding motif of some DNA binding proteins and RNA binding proteins. Several DNA binding modes of the antiparallel β-sheet structure have been proposed: (i) the β-sheet domain of the *Escherichia coli* chromosomal proteins HU or IHF contacts DNA in the minor groove (Yang & Nash, 1989; Churchill & Travers, 1991); (ii) Arc, Mnt, or Met repressor binds to the major groove of the DNA helix with the β-sheet regions (Rafferty et al., 1989; Breg et al., 1990); (iii) the RNA-binding domain of RNP or the gene 5 protein from bacteriophage fd interacts with nucleic acid bases by amino acid residues positioned on the surface of β-sheet regions (Scherly et al., 1990; Hoffman et al., 1991). To our knowledge, the diversity of the binding mode reported on the antiparallel β-sheet has never been observed for other DNA binding motifs such as helix–turn–helix (Pabo & Sauer, 1984), Zn-finger (Evans & Hollenberg, 1988), and leucine zipper (Landschultz et al., 1988). This is the first report on the interaction between DNA and a small peptide that contains an antiparallel β-sheet.

Implication for Antimicrobial Activity of Tachyplesin I. The peptide has been reported to have LPS binding (Nakamura et al., 1988) and phospholipid binding activities (Matsuzaki et al., 1991). Recent studies suggest that one main biological action of other antimicrobial peptides such as defensin (Lehrer & Ganz, 1991) and bactenecin (Frank et al., 1990) derived from animal immunocytes is due to lipid and cell membrane bindings. On the other hand, it is known that several phospholipid binding proteins (bovine lung annexins and human serum lipoproteins) bind tightly to Z-form DNA and that the binding of the *lac* repressor to its operator sequence is inhibited by phospholipid (Krishna et al., 1990). One biologically active compound often has more than two kinds of macromolecule binding activities. Although we must give solid evidence about the DNA binding property of tachyplesin I and its antimicrobial activity, the present result leads to speculation that DNA as well as LPS may be one of the biological targets of tachyplesin I.

Supplementary Material Available

CD spectra of tachyplesin I in the presence or absence of DTT and comparative CD spectra of tachyplesin I and Ala–tachyplesin (2 pages). Ordering information is given on any current masthead page.

References

Akaji, K., Fujii, N., Tokunaga, F., Miyata, T., Iwanaga, S., & Yajima, H. (1989) *Chem. Pharm. Bull. 37*, 2661–2664.
Breg, J. N., van Opheusden, J. H. J., Burgering, M. J. M., Boelens, R., & Kaptein, R. (1990) *Nature 346*, 586–589.
Churchill, M. E. A., & Travers, A. A. (1991) *Trends Biochem. Sci. 16*, 92–97.
Evans, R. M., & Hollenberg, S. M. (1988) *Cell 52*, 1–3.
Fox, K. R., & Waring, M. J. (1984) *Nucleic Acids Res. 12*, 9271–9285.
Frank, R. W., Gennaro, R., Schneider, K., Przybylski, M., & Romeo, D. (1990) *J. Biol. Chem. 265*, 18871–18874.
Galas, D. J., & Schmitz, A. (1978) *Nucleic Acids Res. 5*, 3157–3170.
Harshman, K. D., & Dervan, P. B. (1985) *Nucleic Acids Res. 13*, 4825–4835.

Helene, C., & Dimicoli, J.-L. (1972) *FEBS Lett. 26*, 6-10.
Hertzberg, R. P., & Dervan, P. B. (1982) *J. Am. Chem. Soc. 104*, 313-315.
Hoffman, D. W., Query, C. C., Golden, B. L., White, S. W., & Keene, J. D. (1991) *Proc. Natl. Acad. Sci. U.S.A. 88*, 2495-2499.
Kawano, K., Yoneya, T., Miyata, T., Yoshikawa, K., Tokunaga, F., Terada, Y., & Iwanaga, S. (1990) *J. Biol. Chem. 265*, 15365-15367.
Krishna, P., Kennedy, B. P., Waisman, D. M., van de Sande, J. H., & McGhee, J. D. (1990) *Proc. Natl. Acad. Sci. U.S.A. 87*, 1292-1295.
Kuwahara, J., & Sugiura, Y. (1988) *Proc. Natl. Acad. Sci. U.S.A. 85*, 2459-2463.
Landschultz, W. H., Johnson, P. F., & McKnight, S. L. (1988) *Science 240*, 1759-1764.
Lane, M. J., Dabrowiak, J. C., & Vournakis, J. N. (1983) *Proc. Natl. Acad. Sci. U.S.A. 80*, 3260-3264.
Lehrer, R. I., Ganz, T., & Selsted, M. E. (1991) *Cell 64*, 229-230.
Low, C. M. L., Drew, H. R., & Waring, M. J. (1984) *Nucleic Acids Res. 12*, 4865-4879.
Mascharak, P. K., Sugiura, Y., Kuwahara, J., Suzuki, T., & Lippard, S. J. (1983) *Proc. Natl. Acad. Sci. U.S.A. 80*, 6795-6798.
Matsuzaki, K., Fukui, M., Fujii, N., & Miyajima, K. (1991) *Biochim. Biophys. Acta 1070*, 259-264.
Maxam, A. M., & Gilbert, W. (1980) *Methods Enzymol. 65*, 499-560.
Miyata, T., Tokunaga, F., Yoneya, T., Yoshikawa, K., Iwanaga, S., Niwa, M., Takao, T., & Shimonishi, Y. (1989) *J. Biochem. (Tokyo) 106*, 663-668.
Morita, F. (1974) *Biochim. Biophys. Acta 343*, 674-681.
Nakamura, T., Furunaka, H., Miyata, T., Tokunaga, F., Muta, T., Iwanaga, S., Niwa, M., Takao, T., & Shimonishi, Y. (1988) *J. Biol. Chem. 263*, 16709-16713.
Pabo, C. O., & Sauer, R. T. (1984) *Annu. Rev. Biochem. 53*, 293-321.
Rafferty, J. B., Somers, W. S., Saint-Girons, I., & Phillips, S. E. V. (1989) *Nature 341*, 705-710.
Scamrov, A. V., & Beabealashvilli, R. Sh. (1983) *FEBS Lett. 164*, 97-101.
Scherly, D., Boelens, W., Dathan, N. A., van Venrooij, W. J., & Mattaj, I. W. (1990) *Nature 345*, 502-506.
Siebenlist, U., & Gilbert, W. (1980) *Proc. Natl. Acad. Sci. U.S.A. 77*, 122-126.
Stubbe, J., & Kozarich, J. W. (1987) *Chem. Rev. 87*, 1107-1136.
Sugiura, Y., & Suzuki, T. (1982) *J. Biol. Chem. 257*, 10544-10546.
Tullius, T. D., Dombroski, B. A., Churchill, M. E. A., & Kam, L. (1987) *Methods Enzymol. 155*, 537-558.
Van Dyke, M. W., & Dervan, P. B. (1983) *Nucleic Acids Res. 11*, 5555-5567.
Van Dyke, M. W., & Dervan, P. B. (1984) *Science 225*, 1122-1127.
Van Dyke, M. W., Hertzberg, R. P., & Dervan, P. B. (1982) *Proc. Natl. Acad. Sci. U.S.A. 79*, 5470-5474.
Wang, A. H.-J., Ughetto, G., Quigley, G. J., Hakoshima, T., van der Marel, G. A., van der Boom, J. H., & Rich, A. (1984) *Science 225*, 1115-1121.
Yang, C.-C., & Nash, H. A. (1989) *Cell 57*, 869-880.

Identification of Intermolecular RNA Cross-Links at the Subunit Interface of the *Escherichia coli* Ribosome†

Philip Mitchell,* Monika Osswald, and Richard Brimacombe
Max-Planck-Institut für Molekulare Genetik, Abteilung Wittmann, Ihnestrasse 73, Federal Republic of Germany
Received October 11, 1991; Revised Manuscript Received December 20, 1991

ABSTRACT: ^{32}P-Labeled 70S ribosomes and polysomes were isolated from cultures of *Escherichia coli* and treated with the cross-linking reagent bis(2-chloroethyl)methylamine. Intermolecular 16S-23S RNA cross-linked complexes were separated from other products of the cross-linking reactions by a two-step sucrose density gradient centrifugation procedure and subjected to oligodeoxynucleotide-directed partial nuclease digestions with RNase H. Cross-linked RNA fragments released by such directed digests were resolved by two-dimensional gel electrophoresis and analyzed using classical oligonucleotide fingerprinting techniques. Two distinct intermolecular cross-links between the 16S and 23S RNA could be localized in this manner, involving positions 1408-1411 and 1518-1520 in the 16S RNA sequence and positions 1912-1920 in the 23S RNA sequence. These data provide the first direct topographical links between the RNA of the 30S and 50S subunits in the functional ribosome and, together with previous topographical data concerning the three-dimensional folding of the rRNA, demonstrate that there is a tight cluster at the ribosomal interface both of sites implicated in ribosomal function and of posttranscriptionally modified nucleotides in the rRNA.

The research efforts of this laboratory have been concentrated on the development and application of cross-linking techniques to obtain detailed information concerning the topography of the 16S and 23S RNA in situ in the *Escherichia coli* ribosome. We have previously reported a large number of intra-RNA and RNA-protein cross-link analyses [summarized by Brimacombe et al. (1990a,b)], and these data sets for 16S and 23S RNA, in conjunction with other topographical information, have been incorporated into a model (Brimacombe et al., 1988a) for the detailed three-dimensional structure of the *E. coli* 16S RNA and, more recently, a model (Mitchell et al., 1990) for the tertiary structure of the tRNA binding domain in 23S RNA from *E. coli*, respectively. In a slightly more

† This work was supported in part by a grant from the Deutsche Forschungsgemeinschaft (SFB 9).

0006-2960/92/0431-3004$03.00/0